Available online at www.sciencedirect.com
ScienceDirect
Surface Science 601 (2007) 2756–2761
SURFACE SCIENCE
www.elsevier.com/locate/susc

In-plane and out-of-plane shape transitions of heteroepitaxially self-assembled nanostructures

I. Goldfarb *

Department of Solid Mechanics, Materials and Systems, Faculty of Engineering, University Research Institute for Nanoscience and Nanotechnology, Tel Aviv University, Ramat Aviv, Tel Aviv 69978, Israel

Available online 20 December 2006

Abstract

In this work, shapes and shape transitions of several types of self-assembled heteroepitaxial nanostructures, as observed in in situ scanning tunneling microscopy experiments during growth, are examined in the framework of several equilibrium and kinetic models. In particular, heteroepitaxial $TiSi_2$ and $CoSi_2$ islands on Si(1 1 1) are shown to behave in accordance with generalized Wulff–Kaishew theorem of equilibrium strained and supported crystal shapes. More specifically, these silicide nanocrystals exhibit *out-of-plane* thickening shape transition by increasing their vertical aspect ratio with growth, as long as they are strained, and inverse (flattening) transition upon relaxation by misfit dislocations. On the other hand, heteroepitaxial Ge and $CoSi_2$ islands on Si(0 0 1) are well-known for their *in-plane* anisotropic elongation. Plausible energetic and kinetic reasons for such elongation, based on the unique nucleation features of Ge–hut/Si(0 0 1) and non-planar $CoSi_2$–hut/Si(0 0 1) interface, are discussed.

Keywords: Vapor-phase epitaxy; Self-assembled nanostructures; Surface structure, morphology, roughness, and topography; Surface thermodynamics; Scanning tunneling microscopy; Germanium; Silicides

1. Introduction

It is important to understand the factors that govern shape and size of nanocrystals, self-assembled on surfaces due to strained-layer heteroepitaxial growth, if they are to be used in realistic devices. Simultaneous discovery of strained, crystallographically-perfect nanometric Ge/Si(0 0 1) [1,2] and $In_{0.5}Ga_{0.5}As$/GaAs(1 0 0) [3] three-dimensional (3D) islands has motivated large body of work, mainly due to their potential as building block in futuristic, low-dimensional, quantum photonic and single-electron devices [4].

In their fundamental work, Tersoff, Tromp, and LeGoues have laid the theoretical foundations for understanding strained-layer (Stranski–Krastanow (S–K) and Volmer–Weber (V–W)) nucleation and growth behaviour of self-assembled nanostructures, by showing that at moderate mismatches elastic relaxation of mismatch strain by substrate distortion (due to force density applied by tilted facets), competes with plastic relaxation by misfit dislocations at lower mismatches, and that in cases where the island height growth is kinetically limited – an island exceeding some critical size becomes unstable against anisotropic elongation [5,6]. Many of the major model's conclusions have been experimentally validated, e.g. dependence of the $Si_{1-x}Ge_x$/Si(0 0 1) island size on the square of strain [7], transition of implanted $CoSi_2$/Si(0 0 1) islands from compact to elongated shape at sizes above critical [8], and the formation of strain-relieving pits in the wetting layer even before the islands are formed [9]. Perhaps surprisingly, elongation of Ge/Si(0 0 1) huts in a kinetically-limited regime does not seem to obey the equilibrium elongation model of Tersoff and Tromp [5]. Even more surprising, elongation of epitaxially grown $CoSi_2$/Si(0 0 1) islands is very different from the $CoSi_2$/Si(0 0 1) islands obtained by ion-implantation by Brongersma et al.

* Tel.: +972 3640 7079; fax: +972 3640 7617.
E-mail address: ilang@eng.tau.ac.il

0039-6028/$ - see front matter © 2006 Elsevier B.V. All rights reserved.
doi:10.1016/j.susc.2006.12.042

[8]: while the latter seem to beautifully fit the equilibrium elongation model [5], in the sense that there is a critical $e\alpha_0$ size above which the islands keep elongating in one direction and shrinking back to α_0 in the other, the former do not exhibit these features, although their width grows slower than length. By using anisotropic mismatch of hexagonal rare-earth silicides, Chen et al. [10] have intentionally grown nanowires elongated along the lower-mismatch direction, minimizing the more highly strained parts of the island. However, for more symmetrical, cubic crystals, Jesson et al. [11] and Voigtländer [12] proposed kinetic growth instability models (as an alternative to equilibrium elongation of Tersoff and Tromp [5]), based on the barrier to adatom attachment to a facet or on the facial-layer nucleation barrier due to interaction of steps comprising the vicinal facet, respectively.

On the other hand, if there are no limitations to the island's height growth, according to generalized Wulff–Kaishew theorem the most effective relaxation with increasing volume would be achieved by thickening in the vertical direction, i.e., by growing more upwards than sideways, ultimately resulting in high vertical aspect ratios and sharp crests [13]. Such thickening transition can be accomplished by a replacement of shallow facets by steeper ones, as in Ge/Si(0 0 1) pyramid–dome transition [14–16], and in a similar transition in the InAs/GaAs system [17]. Sharpening of growing strained $TiSi_2$ and $CoSi_2$ islands on Si(1 1 1), followed by reverse (flattening) transition upon strain relaxation by misfit dislocations, shown in this work, is another example.

2. Experimental

The experiments were performed in an ultra-high vacuum (UHV) variable-temperature scanning tunneling microscope (VT–STM), equipped with surface electron diffraction apparata, Auger electron spectrometer, and capable of operation up to 1250 °C by direct-current heating. Si (1 1 1) and (1 0 0) wafers were chemically degreased and cleaned *ex vacuo*, and introduced into the UHV. In UHV (base pressure 1×10^{-8} Pa), after thorough degassing, the oxide was evaporated by repeated flashes at 1150–1200 °C, and the clean Si surface was left to order during a slow cool to the desired temperature, until well-ordered (1 1 1)–(7×7) and (0 0 1)–(2×1) surfaces were observed in diffraction and STM images. Ti and Co for silicide nanostructure growth were evaporated from a precise e-beam evaporator onto Si(1 1 1) at room temperature (RT) and Si(0 0 1) at 500 °C, respectively, mounted at the VT–STM stage, subsequently undergoing a series of annealing treatments in the STM under continuous imaging. Ge was grown on Si(0 0 1) from GeH_4 in a 350–480 °C temperature range, under continuous imaging, as well. STM images were acquired using conventional tunneling conditions of $I = 0.1$–0.2 nA and $-3.0\text{ V} < V < +3.0$ V in a constant-current mode.

3. Results and discussion

3.1. Out-of-plane shape transitions

3.1.1. $TiSi_2$ nanocrystals on Si(1 1 1)

Fig. 1 catches the most important evolution stages of the titanium silicide nanocrystals on Si(1 1 1) with annealing temperature. Up to 500 °C, the shapes of the initially unreacted titanium and then silicide agglomerates, forming a disordered quasi-continuous layer, were difficult to define. At 500 °C (Fig. 1a), even though the appearance is still quite disordered, coalescence and coarsening processes already created tiny but clearly round-shaped nanocrystals. The effect of raising the temperature by 60 °C was even more profound on the nanocrystal shape, size, and density: as can be seen in Fig. 1b, the significant increase in the mean size was followed by similarly significant decrease in the nanocrystal number density and transformation of the round-shaped particles into cone-like ones. However, the cones became more and more truncated upon further annealing at 600 °C and 660 °C (Fig. 1c–d). Considerable increase in the mean nanocrystal size accompanied by disappearance of the small-sized ones and drastic reduction in number density, obvious in Fig. 1, is a clear signature of Ostwald ripening [18,19].

The observed shape transformations of $TiSi_2$ nanocrystals can be accounted for in the framework of generalized Wulff–Kaishew theorem of equilibrium crystal shapes (ECS). The total free energy of lattice-mismatched (strained) formation of heteroepitaxial $TiSi_2$ island of volume "V" on Si surface in a Volmer–Weber mode, is composed of the change due to formation of a solid from supersaturated dilute phase, formation of new surfaces (facets) and interfaces, and, finally, the elastic energy stored in the island/substrate system [13],

$$\Delta G = -\Delta\mu V + \left\{\sum_i \gamma_i A_i + A_{\text{int}}(\gamma_{\text{TiSi}_2} - \beta)\right\} + cV\varepsilon^2 R \qquad (1)$$

where $\Delta\mu$ is the chemical potential difference between dilute and compact phase, γ_i and A_i are the surface energy and area of the i-facet, respectively, γ_{TiSi_2} is the energy of the $TiSi_2$ surface parallel to the substrate, A_{int} is the interface area, and β is the Dupré adhesion term. In the last, strain-related term, c contains the relevant island–substrate elastic constants, ε is mismatch-strain, and (fully relaxed) $0 < R < 1$ (fully strained) is the shape-dependent relaxation factor. A Volmer–Weber nanocrystal of fixed volume and n_i facets inclined by θ_i to the substrate's surface assumes its ECS when all the partial derivatives of ΔG go to zero, resulting in an equilibrium vertical aspect ratio:

$$r_i = \frac{2\gamma_{\text{TiSi}_2} - \beta + cV\varepsilon^2 \frac{\partial R}{\partial A_{\text{int}}}\Big|_{A_i}}{\gamma_i - \gamma_{\text{TiSi}_2}\cos\theta_i + c\varepsilon^2 \frac{V}{n_i}\frac{\partial R}{\partial A_i}\Big|_{A_{\text{int}}}} \qquad (2)$$

Since most of the strain is concentrated at the island/substrate interface region [11,20], extension of the interfacial

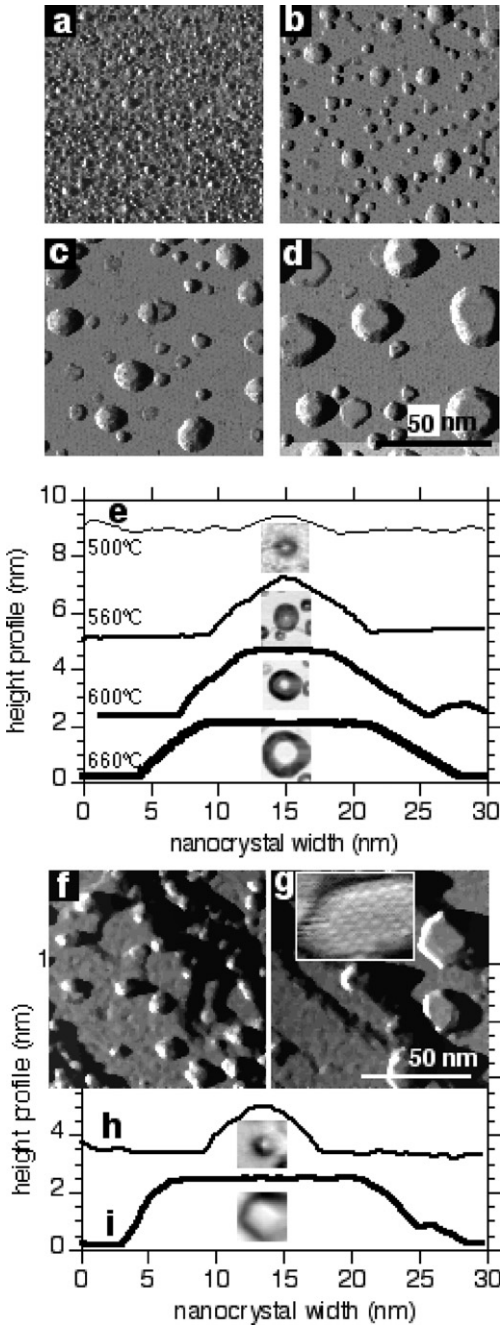

Fig. 1. STM-recorded (current image) various stages of evolution during the anneal of RT-deposited $TiSi_2$/Si(1 1 1) nanocrystals at (a) 500 °C, (b) 560 °C, (c) 600 °C, and (d) 660 °C annealing temperature. (e) Quantitative evaluation of the nanocrystal shape and vertical aspect ratio by cross-sectional STM height profiles, at the same four temperatures. (f), (g) Flattening of $CoSi_2$/Si(1 1 1) nanocrystals with increasing size, and (h), (i) respective cross-sectional height profiles of typical nanocrystals in (f) and (g). Nanocrystal images in the height profile insets were filtered to emphasize slopes, where the flattest portions are the brightest, and darker contrast reflects higher slopes.

area, A_{int}, increases the overall strain and hence the relaxation factor R, whereas the extension of the facet area, A_i, promotes further relaxation and decreases R. In other words, effective relaxation of mismatch strain promotes higher vertical aspect ratios of the growing island, ultimately leading to island's top sharpening [13]. Precisely that was observed in the $TiSi_2$ nanocrystals upon raising the temperature from 500 °C to 560 °C (Fig. 1a–b): the significantly greater volume of the nanocrystals at 560 °C induces higher vertical aspect ratio than at smaller volumes at 500 °C, and even apex sharpening, judged from cross-sectional height profiles in Fig. 1e. This also indicated the strained state of the nanocrystals at that stage. On the other hand, if islands continue to grow, misfit dislocation will be inevitably introduced at the interface, initiating plastic strain relaxation. This is expected to reverse the shape transition from sharpening to flattening by progressive truncation of the island crests [13], as, again, observed in the $TiSi_2$ nanocrystals upon further growth at 600 °C and 660 °C (Fig. 1c–e), implying at least partial strain relaxation at these temperatures. Significant mass transfer required for a retreating top facet is most probably facilitated by step-forming screw dislocations [21].

3.1.2. $CoSi_2$ nanocrystals on Si(1 1 1)

In this respect, $CoSi_2$/Si(1 1 1) nanocrystals show very similar behaviour, as evident in Fig. 1f–i. At small size, most of the nanocrystals are hemispheric (Fig. 1f), as clearly reflected in their typical cross-sectional height profiles shown in Fig. 1h (inset shows the profiled particle in a surface-slope mode). Hence, at this point, it is reasonable to assume coherency between the small fully strained nanoislands and the substrate.

And again, just as in the $TiSi_2$/Si(1 1 1) case, the strain and elastic energy build-up with increasing nanocrystal size (volume), appears to be relieved by misfit dislocations, causing flattening shown in Fig. 1g and i. In this case, a characteristic $CoSi_2$(1 1 1)-(2×2) reconstruction is detected on the flat tops of the nanocrystals by high-resolution STM imaging (see inset in Fig. 1g).

3.2. In-plane shape transitions

While strain relaxation by increased vertical aspect ration is undoubtedly the most effective one, in the kinetically limited regime the island height may not be allowed to grow as fast as the edges. Tersoff, Tromp, and LeGoues [5,6] have analyzed such a case, of a shallow and isolated faceted island of width "s", length "t", height "h", volume "V", and facet inclination angle "θ". By defining $\Gamma = \gamma_{\mathrm{facet}}\operatorname{cosec}\theta - \gamma_{\mathrm{surf}}\cot\theta$, and $c = E_{\mathrm{isl}}^2\varepsilon^2(1-\nu_{\mathrm{sub}})/(2\pi\mu_{\mathrm{sub}})$, they expressed the total free energy of the island as a competition between the surface and strain-relaxation energy.

$$\frac{E_{\mathrm{total}}^{\mathrm{S\text{–}K}}}{V} = 2\Gamma\left(s^{-1}+\frac{s}{A}\right) - 2ch\left\{s^{-1}\ln\left(\frac{se^{\frac{3}{2}}}{h\cot\theta}\right)+\frac{s}{A}\ln\left(\frac{Ae^{\frac{3}{2}}}{sh\cot\theta}\right)\right\} \qquad (3)$$

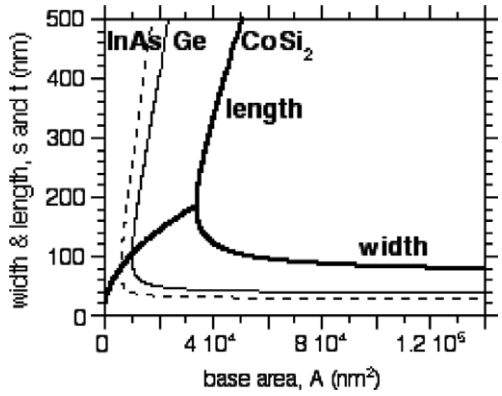

Fig. 2. Theoretical $s,t(A)$ plots for $CoSi_2$/Si(001), Ge/Si(001), and InAs/GaAs(001) nanocrystals, calculated from minimization of Eq. (3) (see text for details).

Minimization of the total free energy density, $E_{total}/V(=hst)$, with respect to s and t, shows equilibrium isotropic growth of the island up to $e\alpha_0 = s = t = h\cot\theta\exp(\Gamma/ch + 1/2)$, and then the island will anisotropically elongate in one direction and shrink to α_0 in the perpendicular direction, since by such optimization it gains at least half of its relaxation energy.

Such equilibrium elongation has been suspected to take place in many heteroepitaxial nanocrystal systems, such as Ge/Si(001) [5], $CoSi_2$/Si(001) [8], (InGa)As/GaAs(001) [22], GaSb/GaAs(001) [23], Er_xSi_y/Si(001) [24], and even $TiSi_2$/Si(111) [25,26]. Using the Tersoff–Tromp model, an equilibrium width-to-length, s/t, ratio as a function of the island base, $A = st$, can be found at every growing size, by expressing dimension s or t as a function of A, and minimizing E_{total}/V with respect to the other dimension [5]. This $s,t(A)$ plot is in the shape of a fork, bifurcating at $e\alpha_0$, with the length growing further and width decaying back to α_0, as plotted using typical heights, facet angles, elastic constants and surface energies for $CoSi_2$/Si(001) [8], Ge/Si(001) [27,28], and InAs/GaAs(001) [22] in Fig. 2.

3.2.1. Ge nanocrystals on Si(001)

The experimental curves, though, do not seem to agree with the theoretical predictions: in most cases the transition size, $e\alpha_0$, is many times or even orders of magnitude smaller than the predicted one, and island width usually merely slows down rather than shrinking back to α_0, as shown in Figs. 3 and 4, for Ge/Si(001) and $CoSi_2$/Si(001), respectively.

Due to exponential dependence of α_0 on Γ/ch, many factors may drastically change the α_0 value. For example, since surface energies are mostly obtained from calculations [20,27], they can quite significantly vary depending on the calculation method and the assumption used. Hence, Γ, which reflects the difference between facet and flat surface energy, can assume arbitrarily low and even negative values, resulting, in turn, in correspondingly low α_0. For example, using the relevant Si–Ge mismatch and

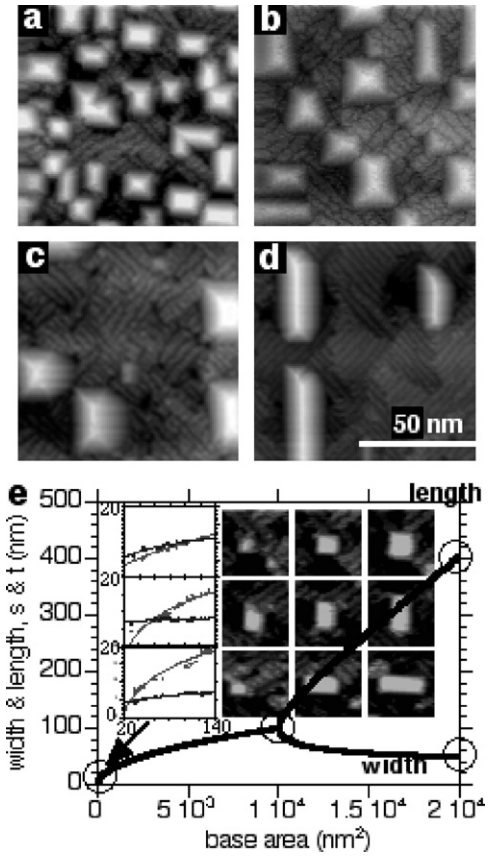

Fig. 3. STM topographs recorded in situ during Ge/Si(001) growth at (a) 360 °C, (b) 420 °C, (c) 450 °C, and (d) 480 °C temperatures. (e) Experimental $s,t(A)$ plots for three individual huts growing at 360 °C (shown on the right), superposed on the theoretical $s,t(A)$ plot calculated from Eq. (3), where the arrow indicates an approximate position of the experimental bifurcation point, $e\alpha_0$, on the scale of the calculated plot.

elastic constants, and experimentally measured Ge hut height, h, facet angle, θ, and transition size, α_0, Voigtländer obtained $\Gamma = -0.68\ \text{meV/Å}^2$, rather than the theoretical value of $+1.6\ \text{meV/Å}^2$ [12]. One of the possible reasons for the discrepancy could be the assumption of non-interacting islands, which may not hold in high-density arrays shown in Fig. 3a, where Ge huts are clearly seen to impinge on one another. However, this assertion was not experimentally supported by the studies of sparse Ge hut arrays (obtained by a deliberate suppression of hut nucleation at higher growth temperatures): in fact, length-to-width ratios, t/s, were higher in the most dilute arrays at 480 °C (Fig. 3d) than in the most dense ones at 360 °C (Fig. 3a), perhaps, simply due to lower probability for impingement. Furthermore, there is another discrepancy, namely, the hut width (while grows much slower than the length) never actually shrinks (see the experimental length and width curves in the inset of Fig. 3e), as expected from the Tersoff–Tromp model.

It is more likely that pits (dark depressions adjacent to the huts in Fig. 3a and in the inset of Fig. 3e) and step edges, that serve as the nucleation centers for the Ge huts

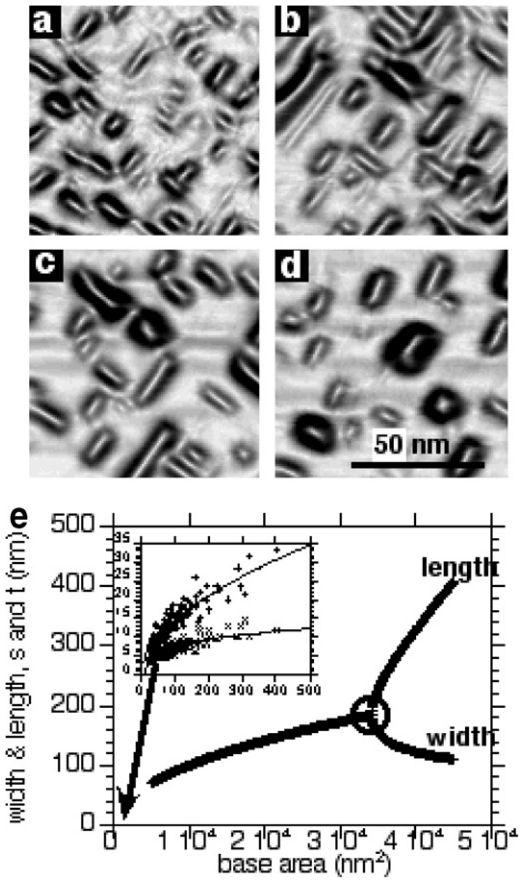

Fig. 4. STM topographs recorded in situ during isothermal annealing of $CoSi_2$/Si(001) nanocrystals at 500 °C for (a) 1 h, (b) 18 h, (c) 66 h, and (d) 111 h. The images were slope-filtered, to better distinguish between flat (bright) and inclined (dark) regions. (e) Experimental $s,t(A)$ plot superposed on the theoretical one calculated from Eq. (3), where the arrow indicates an approximate position of the experimental bifurcation point, $e\alpha_0$, on the scale of the calculated plot.

in the low-temperature ($T < 550$ °C) kinetically limited regime [9], modify the local energetics of the hut in a way not taken into account in the Tersoff–Tromp model [5]. Since the huts form by agglomeration of the material transferred from the pits, there is at least one hut facet in contact with that of the pit, breaking the energetic degeneracy of the hut facets. By introducing such an edge anisotropy, $\beta^2 = \gamma_s/\gamma_t$ (where $\gamma_s \neq \gamma_t$ are the surface energy densities of the short and long mutually perpendicular hut facets), Li, Liu, and Lagally have shown, that upon exceeding a critical diameter for isotropic–anisotropic growth transition, D_c, the pyramid will elongate in a single most probable direction that maximizes the size of the low-energy edge, contrary to the isotropic case, where each of the two possible ⟨100⟩ elongation directions is equally probable [29]. {Strictly speaking, they analyzed two-dimensional rectangular island of width "s" and length "t" (therefore of diameter $D = (st)^{1/2}$, perimeter $P = 2(s + t)$, and aspect ratio $c^2 = s/t$), however this analysis can be successfully applied to three-dimensional islands by replacing edges with facets, lengths with areas, edge-energies with surface energies, and force monopoles due to island periphery by monopoles due to tilted facets}. Another important factor that affects the island shape is the relative strength of the edge (facet) to strain energies, $\alpha = (\gamma_s\gamma_t)^{1/2}/E_s$, where $E_s = F^2(1+\nu)/(2\pi\mu)$ and F is the force monopole. The critical diameter, D_c, is obtained from minimization of the total free energy, E_{total} [29],

$$E_{total} = E_s\left\{P\left[\alpha\frac{\beta^2c^2+1}{\beta^2c^2+\beta} + G(c)\right] - 2P(1-\nu)\ln\frac{D}{a_0}\right\} \qquad (4)$$

where $G(c)$ is a complex function of aspect ratio only, and a_0 is in the order of a surface lattice constant), and for strongly anisotropic facet energies can be arbitrarily small, as indeed observed in Ge/Si(001) huts!

3.2.2. $CoSi_2$ nanocrystals on Si(001)

In certain respects, this case is even more complex than that of Ge/Si(001), and not only due to the chemical Co–Si reaction. Because it is a V–W (rather than S–K) system, interfacial energy, γ_{inter}, has to be taken into account, and accordingly $\Gamma = \gamma_{facet}\mathrm{cosec}\,\theta - (\gamma_{top} + \gamma_{surf} - \gamma_{inter})\cot\theta/2$, and E_{total}/V changes to:

$$\frac{E^{V\text{–}W}_{total}}{V} = 2\Gamma\left(s^{-1} + \frac{s}{A}\right) + h^{-1}(\gamma_{inter} + \gamma_{top} - \gamma_{surf}) - 2ch\left\{s^{-1}\ln\left(\frac{se^{\frac{3}{2}}}{h\cot\theta}\right) + \frac{s}{A}\ln\left(\frac{Ae^{\frac{3}{2}}}{sh\cot\theta}\right)\right\} \qquad (5)$$

However, the additional and related complication stems from the well known fact, that the interface between the $CoSi_2$ huts and Si(001) is usually not flat, but rather grooved [30]. While this can explain the ⟨110⟩ elongation directions (that are naturally formed by intersection of the {111}-groove facets) [30], the driving force for the elongation is still not clear. Yet, unlike the case of Ge/Si(001) huts, the discrepancy between the behaviour of $CoSi_2$/Si(001) huts and the equilibrium Tersoff–Tromp model, may well have to do with the hut density and resulting hut–hut interactions neglected in the model. By creating sparse distribution of well separated $CoSi_2$ huts using ion-implantation, rather than the epitaxial, impinging ones shown in Fig. 4, Brongersma et al. [8] have obtained excellent fit to the bifurcating Tersoff–Tromp equation (5) [5], shown as the outermost curve in Fig. 2. Smaller lateral aspect ratios, and thus more symmetric shapes of the dense epitaxial $CoSi_2$ huts after a prolonged anneal at 500 °C (Fig. 4d), may well indicate that the initially elongated hut shape is not the most energetically favored shape for them, contrary to the sparse ones obtained by ion implantation.

4. Conclusions

Out-of-plane shape transitions of heteroepitaxial $TiSi_2$/Si(111) and $CoSi_2$/Si(111) nanocrystals, and in-plane transitions of Ge/Si(001) and $CoSi_2$/Si(001) nanocrystals, were in situ monitored with STM and analyzed. Sharpening and flattening transitions in the silicide nanocrystals

on Si(1 1 1) are shown to conform to the expected from generalized Wulff–Kaishew theorem of equilibrium strained and supported crystal shapes. As long as they are strained, growing elastic strain energy induces sharpening shape transition by increasing vertical aspect ratio, whereas inverse (flattening) transition is caused by relaxation due to misfit dislocations. The discrepancy between the elongation behaviour of Ge/Si(0 0 1) huts and equilibrium models (e.g. by Tersoff and Tromp), may stem from the anisotropic hut facet energies due to the presence of pits where the huts were nucleated. It is not inconceivable, that a hut facet adjacent to a pit will differ in energy from the other facets, facilitating elongation directions that minimize the total energy. Anisotropic elongation of heteroepitaxial $CoSi_2$/Si(0 0 1) nanohuts differs from equilibrium elongation of larger $CoSi_2$/Si(0 0 1) huts obtained by ion implantation, apparently due to non-negligible nanohut–nanohut interactions in the former, and is probably not an equilibrium one, since more symmetric shape was recovered by a prolonged high-temperature anneal.

Acknowledgements

The authors wish to acknowledge the generous contribution of the Israel Science Foundation (ISF GR 9043/00) towards the equipment costs.

References

[1] D.J. Eaglesham, M. Cerullo, Phys. Rev. Lett. 64 (1990) 1943.
[2] Y.-W. Mo, D.E. Savage, B.S. Swartzentruber, M.G. Lagally, Phys. Rev. Lett. 65 (1990) 1020.
[3] S. Guha, A. Madhukar, K.C. Rajkumar, Appl. Phys. Lett. 57 (1990) 2110.
[4] V.A. Shchukin, N.N. Ledentsov, D. Bimberg, Epitaxy of Nanostructures, Springer-Verlag, Berlin, Heidelberg, 2004.
[5] J. Tersoff, R.M. Tromp, Phys. Rev. Lett. 70 (1993) 2782.
[6] J. Tersoff, F.K. LeGoues, Phys. Rev. Lett. 72 (1994) 3570.
[7] W. Dorsch, H.P. Strunk, H. Wawra, G. Wagner, J. Groenen, R. Carles, Appl. Phys. Lett. 72 (1998) 179.
[8] H. Brongersma, M.R. Castell, D.D. Perovic, M. Zinke-Allmang, Phys. Rev. Lett. 80 (1998) 3795.
[9] I. Goldfarb, P.T. Hayden, J.H.G. Owen, G.A.D. Briggs, Phys. Rev. Lett. 78 (1997) 3959.
[10] Y. Chen, D.A.A. Ohlberg, R.S. Williams, J. Appl. Phys. 91 (2002) 3213.
[11] D.E. Jesson, G. Chen, K.M. Chen, S.J. Pennycook, Phys. Rev. Lett. 80 (1998) 5156.
[12] B. Voigtländer, Surf. Sci. Rep. 43 (2001) 127.
[13] P. Muller, R. Kern, Surf. Sci. 457 (2000) 229.
[14] G. Medeiros-Ribeiro, A.M. Bratkovski, T.I. Kamins, D.A.A. Ohlberg, R.S. Williams, Science 279 (1998) 353.
[15] F.M. Ross, R.M. Tromp, M.C. Reuter, Science 286 (1999) 1931.
[16] F. Montalenti, P. Raiteri, D.B. Migas, H. von Känel, A. Rastelli, C. Manzano, G. Costantini, U. Denker, O.G. Schmidt, K. Kern, L. Miglio, Phys. Rev. Lett. 93 (2004) 216102.
[17] G. Costantini, A. Rastelli, C. Manzano, R. Songmuang, O.G. Schmidt, K. Kern, H. von Känel, Appl. Phys. Lett. 85 (2004) 5673.
[18] I. Goldfarb, P.T. Hayden, J.H.G. Owen, G.A.D. Briggs, Phys. Rev. B 56 (1997) 10459.
[19] I. Goldfarb, S. Grossman, G. Cohen-Taguri, Appl. Surf. Sci. 252 (2006) 5355.
[20] O.E. Shklyaev, M.J. Beck, M. Asta, M.J. Miksis, P.W. Voorhees, Phys. Rev. Lett. 94 (2005) 176102.
[21] I. Goldfarb, G. Cohen-Taguri, S. Grossman, M. Levinshtein, Phys. Rev. B 72 (2005) 075430.
[22] W. Ma, R. Nötzel, H.-P. Schönherr, K.H. Ploog, Appl. Phys. Lett. 79 (2001) 4219.
[23] B.M. Kinder, E.M. Goldys, Appl. Phys. Lett. 73 (1998) 1233.
[24] L. Fitting, M.C. Zeman, W.-C. Yang, R.J. Nemanich, J. Appl. Phys. 93 (2003) 4180.
[25] W.-C. Yang, H. Ade, R.J. Nemanich, J. Appl. Phys. 95 (2004) 1572.
[26] H.F. Hsu, T.F. Chiang, H.C. Hsu, L.J. Chen, Jap. J. Appl. Phys. 43 (7B) (2004) 4541.
[27] G.-H. Lu, F. Liu, Phys. Rev. Lett. 94 (2005) 176103.
[28] K.C. Lin, Y.H. Chiu, J.H. Lin, W.W. Pai, Nanotechnology 16 (2005) S63.
[29] A. Li, F. Liu, M.G. Lagally, Phys. Rev. Lett. 85 (2000) 1922.
[30] Z. He, D.J. Smith, P.A. Bennett, Phys. Rev. Lett. 93 (2004) 256102.